Crystallization and Morphology of Reactor-Made Blends of Isotactic Polypropylene and Ethylene–Propylene Rubber

Y. YOKOYAMA,* T. RICCO

University of Trento, Department of Materials Engineering, Via Mesiano 77, 138050 Trento, Italy

Received 1 November 1996; accepted 12 December 1996

ABSTRACT: The crystallization and morphology of reactor-made blends of isotactic polypropylene (PP) with a large content of ethylene–propylene rubber (EPR) (i.e., $> 50\%$) were investigated. In the blends, PP was found to form spherulites during the crystallization process, with the growth rate constant under isothermal conditions. For crystallization temperatures in the range of 118–152°C, the birefringence of the spherulites varied from negative to positive by decreasing crystallization temperature, while homopolypropylene (homo-PP), the same as used in the blends as a matrix, showed negative spherulites in the whole temperature range investigated (118–152°C). Both the spherulite growth rate and the overall crystallization rate were slower for the blends than for homo-PP. The density of the crystallization nuclei was lower in the blends than in the homo-PP. It was concluded that a large amount of EPR content in the reactor-made blends of PP retards and hinders the crystallization of the matrix. © 1997 John Wiley & Sons, Inc. J Appl Polym Sci **66:** 1007–1014, 1997

Key words: polypropylene blends; crystallization; morphology

INTRODUCTION

Heterophasic copolymers of polypropylene have been produced as toughened grades of isotactic polypropylene (PP). With the aim of further increasing the fracture toughness of PP (or flexible PP, i.e., elastomerlike materials) melt-compounding of PP blends with additional elastomers was necessary. Recently, such kinds of blends have been obtained by polymerization of the monomers directly in the reactor.[1,2] By using this versatile process, it was possible to produce blends with a very high amount of ethylene–propylene rubber (EPR), > 50 wt %, maintaining a heterophasic structure with the matrix of PP embedding the dispersed EPR particles.

The crystallization and morphology of melt blends of PP and EPR have been studied previously[3–8,10,11] and reviewed[12–14] for elastomer contents < 40 wt %. In the present article the crystallization and morphology of reactor-made PP/EPR blends with EPR concentration > 50 wt % were investigated.

EXPERIMENTAL

The materials studied, kindly supplied by Montell Polyolefins (G. Natta Research Centre, Ferrara, Italy), consist of two rubber-modified PP (samples B and C) and a homo-PP (sample A) as a reference. Some main characteristics of the materials are reported in Table I. The blends were made by sequential polymerization in a multistage reactor where the PP polymerization was followed by the EPR copolymerization. Since the materials were synthesized by using the same catalyst and process, the chemical structures, such as isotacticity and molecular weight distribution of PP in samples A, B, and C, should be the same. The matrix of B exactly corresponds to A, and that

Correspondence to: T. Ricco.
* On leave from Showa Denko K. K., 2 Oaza Nakanosu, Oita 870-01, Japan.

Journal of Applied Polymer Science, Vol. 66, 1007–1014 (1997)
 CCC 0021-8995/97/061007-08

Table I Characterization of the Materials

Code	MFR of Matrix (dg/min)	EPR Content (wt %)	C3 in EPR (wt %)	M_w of EPR
A[a]	15	0	—	—
B[b]	15	70	70	430,000
C[b]	8	60	49	430,000

[a] Isotactic homo-PP.
[b] Reactor-made blend of isotactic homo-PP/ethylene–propylene copolymer.

of C is very similar with a small difference in melt flow rate (MFR). The EPR concentration and propylene monomer incorporation in EPR is higher in B than in C. The reactor-made blends and homo-PP were mixed after synthesis with ~ 0.2 wt % stabilizing additives (calcium stearate, phenolic and phosphite stabilizers), and pelletized.

DSC experiments were carried out by a Mettler TC10A instrument (cell type DSC30). The samples, taken from 20-μm-thick films obtained by compression-molding small amounts of material at 210°C for 5 min, were heated to 230°C for 2 min and then quickly cooled, at a rate of 100°C/min, to the predetermined crystallization temperature, T_c. The whole procedure was carried out in a dry nitrogen atmosphere. Before DSC measurements were taken, all the samples were inspected by optical microscopy to check for the existence of unexpected impurities.

Polarized optical microscopy observations

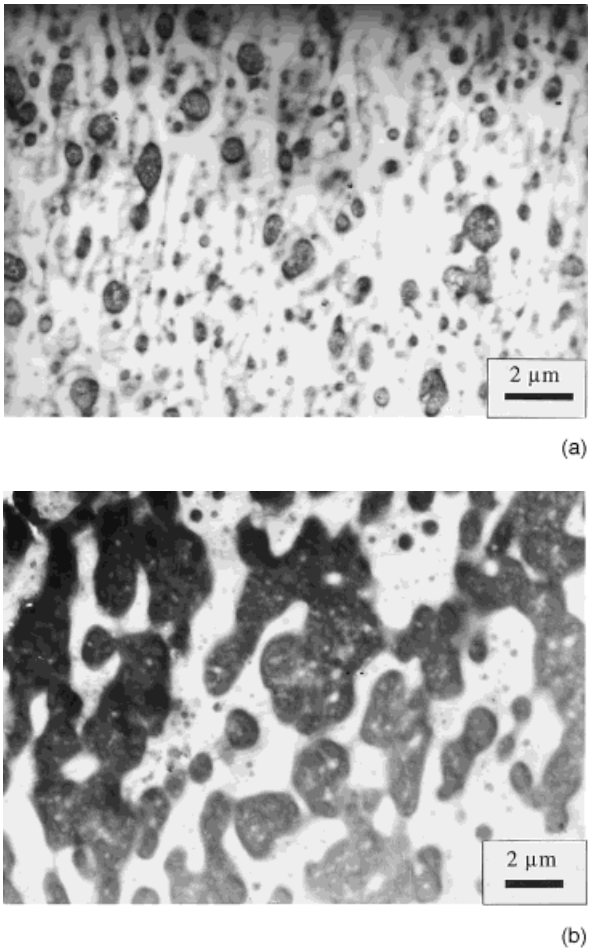

Figure 1 TEM micrographs of ultramicrotomed and RuO_4 stained sections of (a) sample B and (b) sample C.

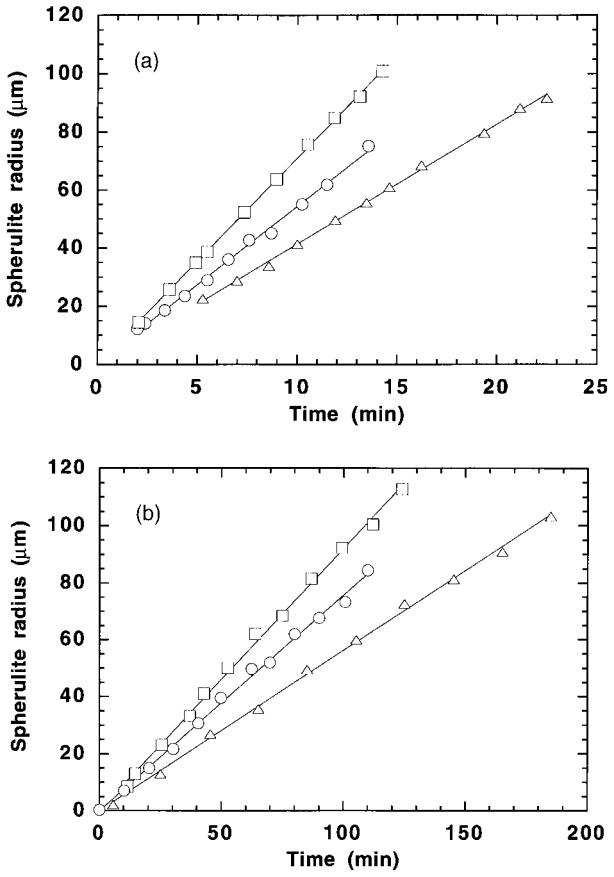

Figure 2 Time course of spherulite radius at the crystallization temperatures of (a) 132°C and (b) 142°C: (□) sample A, (○) sample B, and (△) sample C.

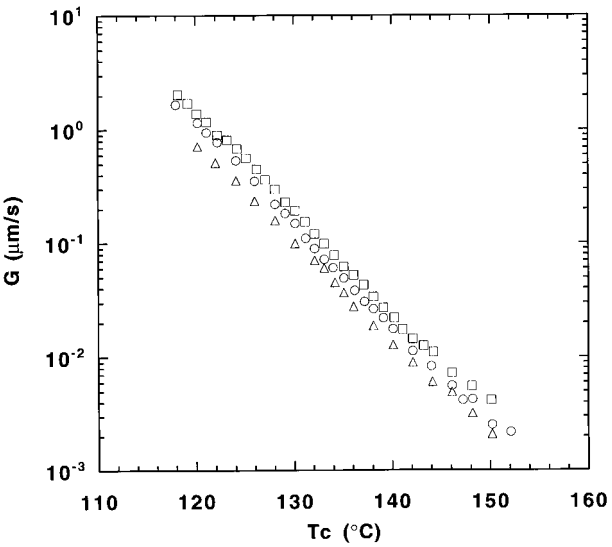

Figure 3 Linear spherulite growth rate, G, versus crystallization temperature: (□) sample A, (○) sample B, and (△) sample C.

were carried out by ORTHLUX II POL-BK microscopy by Leitz and a hot-stage LINKAM Scientific Instruments HFS 91 in a dry nitrogen atmosphere. The samples, cut from 20-μm-thick films obtained by compression molding under the conditions indicated above, were heated to 230°C for 2 min, and then cooled to a predetermined crystallization temperature, T_c, at a rate of 100°C/min. After the thermal equilibrium was reached in the hot stage, the spherulite growth was recorded by a video system. By using PERTEL MET1 image analyzing software the spherulite radii were measured, playing back the video image at different time intervals. The spherulite growth rate was calculated by the slope of the spherulite radius versus time plot. At any given T_c examined, from three to eight different spherulites were considered, and the average value of the spherulite growth rate, G, was calculated. The birefringence sign of the spherulites was observed by using a λ-plate.

TEM observations were also performed on cryogenic ultramicrotomed surfaces, previously stained by RuO_4 at 30°C for 4 h.

RESULTS AND DISCUSSION

TEM photos of the blends are shown in Figure 1. The amorphous part, mainly constituted by EPR, is observed as dark zones because the samples were stained by RuO_4. In both blends PP forms a continuous phase. In blend B, EPR forms a discontinuous phase with finely dispersed particles of submicron dimensions. Also, blend C contains

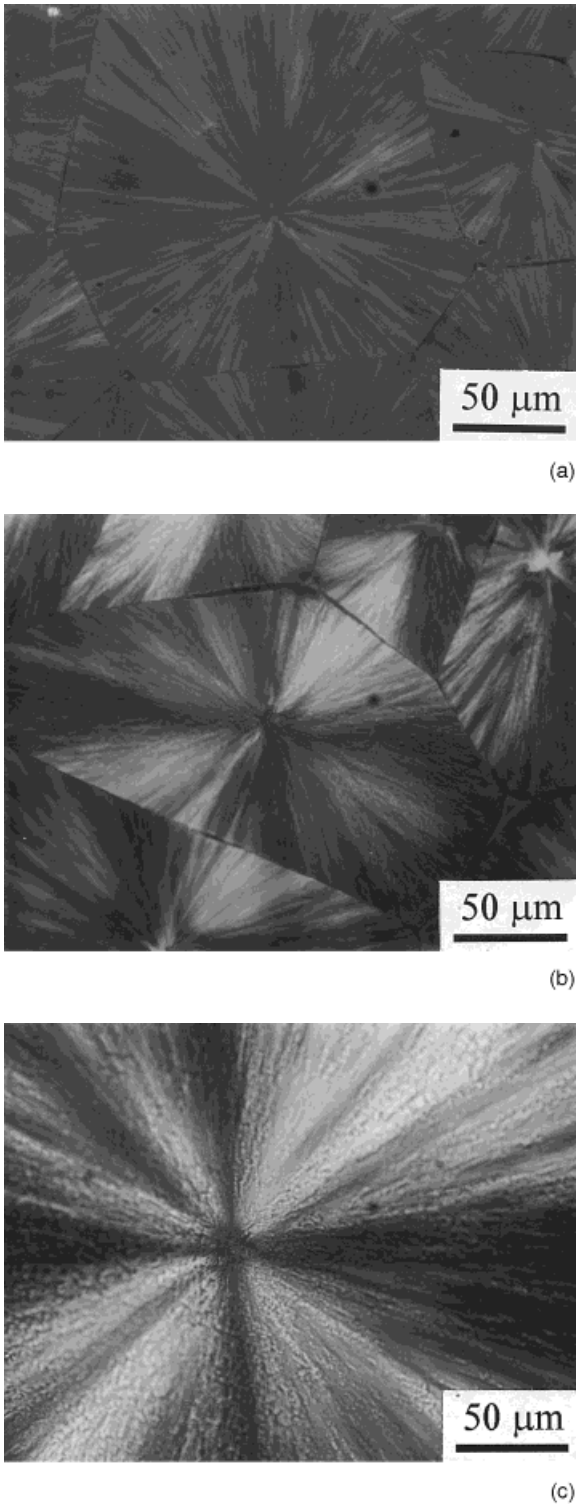

Figure 4 Polarized optical micrographs for sample A (homo-PP) crystallized at (a) 126°C, (b) 136°C, and (c) 145°C.

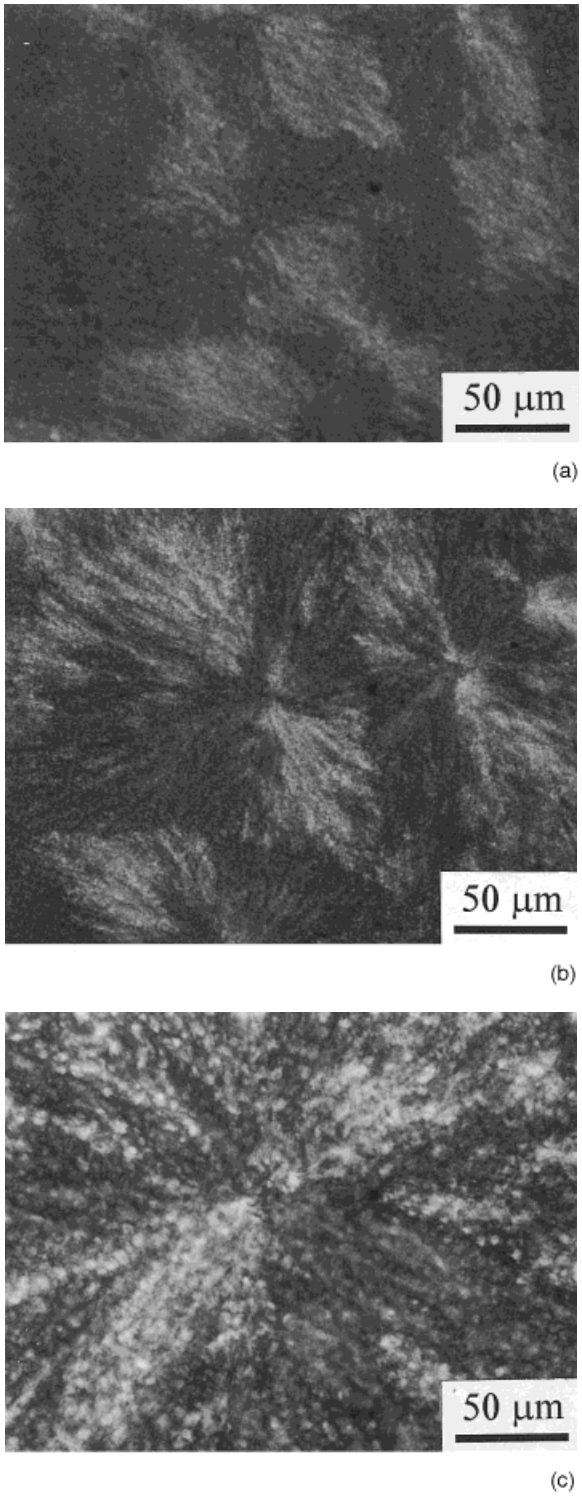

Figure 5 Polarized optical micrographs for sample B (rubber-modified PP) crystallized at (a) 126°C, (b) 136°C, and (c) 152°C.

finely dispersed EPR particles with diameters on the order of micrometers, although EPR seems to form a continuous phase too. In this sample the polyethylene crystalline portion of EPR appears occluded inside the EPR amorphous part.

In all the samples examined that were crystal-

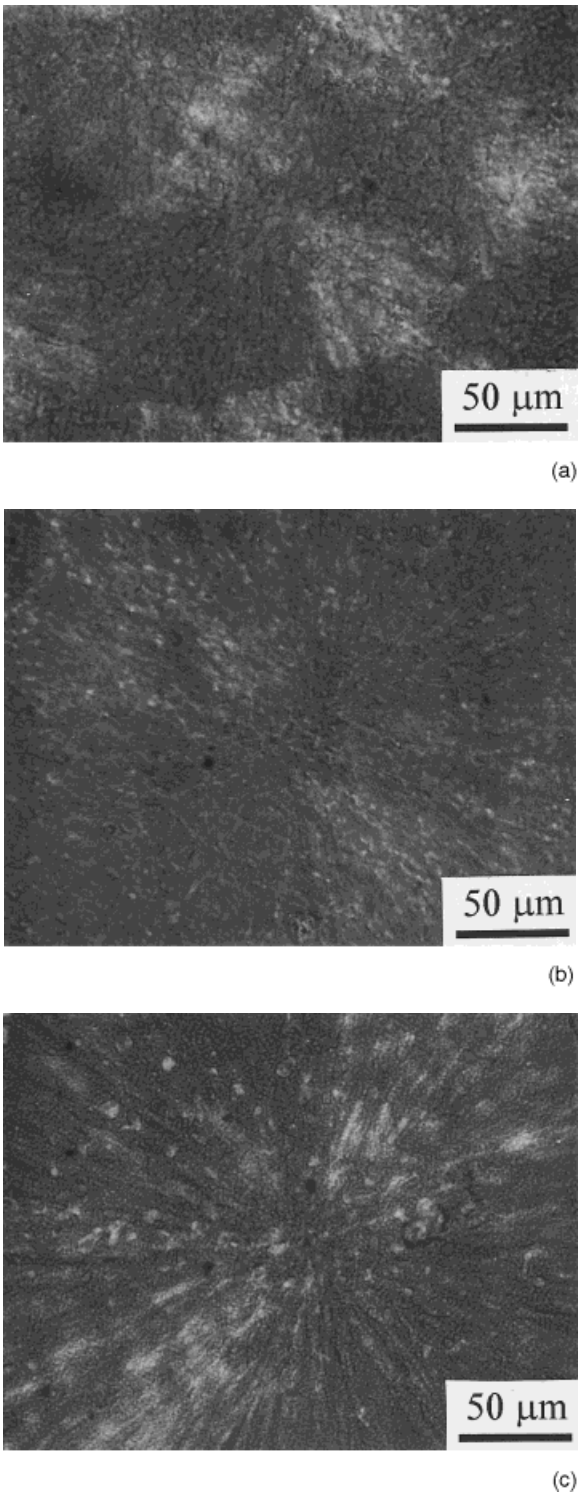

Figure 6 Polarized optical micrographs for sample C (rubber-modified PP) crystallized at (a) 126°C, (b) 136°C, and (c) 144°C.

Table II Spherulite Characterization

Spherulite Type	I	Mixed		II	III	IV
Crystal structure	α	α	α	α	β	β
Sign of birefringence	+	+	−	−	−	−
T_c (°C) (sample A)	n.r.	n.r.	≤ 126	$126 <$	≤ 122	n.r.
T_c (°C) (sample B)	≤ 147	140–147	$148 <$	$150 <$	≤ 120	n.r.
T_c (°C) (sample C)	≤ 136	136–137	138–140	$140 <$	≤ 122	n.r.

n.r., not recognized.

lized from the melt, PP formed spherulites. For these materials typical plots of the spherulite radius as a function of time are shown in Figure 2 at two different crystallization temperatures. These plots are straight lines, as was previously obtained for PP/EPR melt blends[3]: no non-linear behavior is observed within the whole temperature range investigated. The growth rate of the spherulites, G, is shown in Figure 3 as a function of T_c for the three materials. Typically, it appears to decrease with increasing T_c, while at each T_c the spherulite growth rate for samples A and B is always faster than for sample C. The theory[8] predicts that, in phase-separated blends, G decreases by increasing the concentration of the dispersed amorphous phase and by decreasing the particle size. In the present study the spherulite growth rate of the two blends is always slower than that of homo-PP, although in blend B, which has finer particles and a higher rubber concentration, the spherulites grow faster than in blend C. This contradiction with the theory might be explained by the discontinuity of the PP phase in sample C, as can be observed in Figure 1(b). Due to the higher tortuousity of the PP matrix in sample C, the time to fill the space by the growing crystal could be longer and, thus, the spherulite growth rate should be slower.

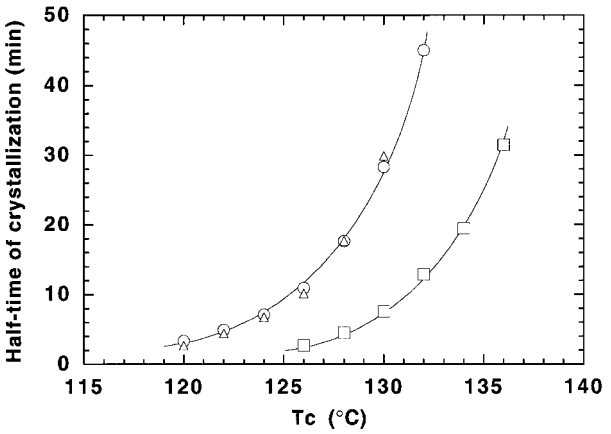

Figure 7 Half-time of crystallization versus crystallization temperature: (□) sample A, (○) sample B, and (△) sample C.

For materials A, B, and C the typical spherulite morphology, observed by polarized optical microscopy at three different temperatures, is shown in Figures 4–6. The dimensions of the spherulites are found to decrease by increasing the crystallization temperature in all the materials studied. In the blends, inclusions of the elastomer within the spherulites can be observed: these inclusions appear finer in sample B than in sample C.

Structural differences of the spherulites are found among the different materials and for each material at the different crystallization temperatures. The main structural characteristics of the spherulites are summarized in Table II. For the homo-PP the crystal structure is typically α, and β-spherulites appear only for $T_c < 122$°C. According to the classification of Padden and Keith,[15] the β-spherulites are of type III, whereas the α-spherulites are of type II and of mixed type for $T_c < 126$°C and $T_c \leq 126$°C, respectively. For the blends the crystalline structure is also typically α, although the presence of β-spherulites of type III is recognized at temperatures < 120–122°C. In particular, the α-spherulites are type II at high temperatures, $T_c > 150$°C for sample B, and $T_c > 140$°C for sample C, and type I for temperatures < 147°C and 140°C for sample B and C, respectively. However, these morphology changes are not sharp and clear, since the presence of the rubber makes it difficult to recognize exactly the spherulitic structure.

In homo-PP the sign of the birefringence is negative over the whole range of temperatures explored, whereas in both the blends a transition of the sign of the spherulite birefringence is found at high temperatures ($\sim$ 148–150°C for sample B, and 138–140°C for sample C). The birefringence change in PP spherulites is known to come from

Table III Parameters of the Crystallization Kinetics and Density of the Crystallization Nuclei for Isothermally Crystallized Homo-PP

T_c (°C)	Avrami Exponent (n)	Rate Constant K (min^{-n})	Spherulite Growth Rate G (μm/s)	Density of Crystallization Nuclei N ($1/\mu\text{m}^3$)
126	2.45	6.05×10^{-2}	4.51×10^{-1}	3.89×10^{-7}
128	2.55	1.52×10^{-2}	2.98×10^{-1}	3.06×10^{-7}
130	2.72	2.77×10^{-3}	1.93×10^{-1}	2.37×10^{-7}
132	2.78	2.75×10^{-4}	1.20×10^{-1}	2.02×10^{-7}
134	2.51	3.91×10^{-4}	7.84×10^{-2}	2.04×10^{-7}
136	2.58	9.58×10^{-5}	5.25×10^{-2}	1.59×10^{-7}

Data are for sample A.

the change of the tangential (T-) to radial (R-) lamellae ratio within the spherulites.[16–19] An increase of T-lamellae induces an increase of the birefringence, while zero birefringence was estimated to occur when the content of T-lamellae is approximately one-third of the total spherulitic branches.[20] Generally, for isothermal crystallization the increase of the crystallization temperature produces a monotonic increase of the cross-hatching density, and the spherulites become negative.[21] The absence of this transition for homo-PP, in disagreement with the results of Padden and Keith[6] who found this transition at 134–138°C, could be justified by hypothesizing a higher degree of isotacticity in our materials that hinders the formation of T-lamellae. The results obtained for the blends would indicate that the sequential polymerization of a large amount of EPR increases the chance of T-lamellae formation, which therefore should be higher for sample B.

The isothermal crystallization rates were evaluated from DSC experiments carried out under conditions of isothermal crystallization. To compare the overall crystallization rate for the three materials studied, the half-time of crystallization, $t_{1/2}$, which is the time corresponding to the 50% crystalline conversion, is plotted against T_c in Figure 7. With increasing T_c, $t_{1/2}$ increases, that is, the overall crystallization rate becomes slower. Homo-PP always crystallizes faster than the blends, which show the same behavior in the temperature range investigated.

The density of the crystallization nuclei can be evaluated from the crystallization kinetics, which are known to be governed by Avrami's equation:

$$1 - \Phi(t) = \exp(-Kt^n) \tag{1}$$

where n is the Avrami's exponent, K the kinetics constant, and $\Phi(t)$ the crystalline conversion at time t. This term is given by the following relationship:

$$\Phi(t) = \frac{\int_0^t (dH/dt)\, dt}{\int_0^{t^\infty} (dH/dt)\, dt} \tag{2}$$

Table IV Parameters of the Crystallization Kinetics and Density of the Crystallization Nuclei for Isothermally Crystallized Rubber-Modified PP

T_c (°C)	Avrami Exponent (n)	Rate Constant K (min^{-n})	Spherulite Growth Rate G (μm/s)	Density of Crystallization Nuclei N ($1/\mu\text{m}^3$)
120	2.48	3.53×10^{-2}	1.15×10^{0}	1.26×10^{-8}
122	2.36	1.62×10^{-2}	7.79×10^{-1}	1.24×10^{-8}
124	2.24	8.74×10^{-3}	5.36×10^{-1}	1.27×10^{-8}
126	2.30	2.85×10^{-3}	3.52×10^{-1}	1.23×10^{-8}
128	2.34	8.63×10^{-4}	2.20×10^{-1}	1.21×10^{-8}
130	2.40	2.29×10^{-4}	1.50×10^{-1}	9.45×10^{-9}
132	2.38	8.33×10^{-5}	9.01×10^{-2}	1.07×10^{-8}

Data are for sample B.

Table V Parameters of the Crystallization Kinetics and Density of the Crystallization Nuclei for Isothermally Crystallized Rubber-Modified PP

T_c (°C)	Avrami Exponent (n)	Rate Constant K (min^{-n})	Spherulite Growth Rate G (μm/s)	Density of Crystallization Nuclei N ($1/\mu\text{m}^3$)
120	2.68	5.08×10^{-2}	7.14×10^{-1}	1.08×10^{-7}
122	2.79	7.91×10^{-3}	5.14×10^{-1}	4.52×10^{-8}
124	2.59	5.03×10^{-3}	3.59×10^{-1}	5.19×10^{-8}
126	2.52	2.07×10^{-3}	2.35×10^{-1}	5.42×10^{-8}
128	2.57	4.36×10^{-4}	1.59×10^{-1}	3.34×10^{-8}
130	2.56	1.17×10^{-4}	9.98×10^{-2}	2.82×10^{-8}

Data are for sample C.

where dH/dt is the heat flow during the crystallization process. Assuming that the nucleation occurs instantaneously, and taking into account the approximation of Kowalewski and Galeski,[22] the density of the crystallization nuclei, N, is given by the following equation:

$$4/3\pi NG^3 = K^{3/n} \quad (3)$$

For a given crystallization temperature, by the evaluation of dH/dt, that can be made directly from the DSC experiments, it is possible to estimate the term $\Phi(t)$, and hence the values of n, K, and N.

The results, obtained at different crystallization temperatures, are reported in Tables III–V for the three materials investigated; N is also plotted as a function of the crystallization temperature in Figure 8. It results to be higher in the homo-PP than in the rubber-modified samples, whereas in sample B it is lower than in sample C. This last finding agrees with the observations made on melt blends,[4,6] which indicates that the dimensions of the spherulites are proportional to the C3-content in EPR.

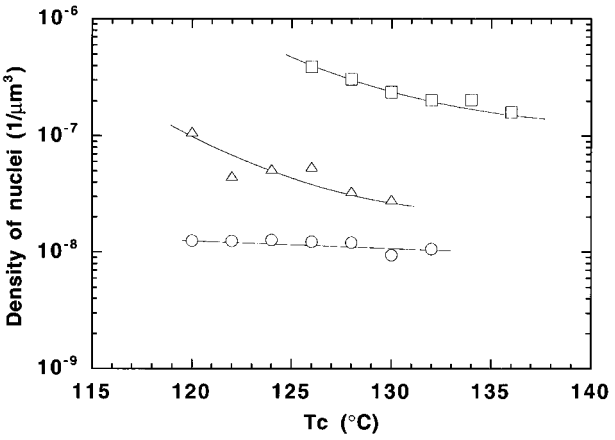

Figure 8 Density of the crystallization nuclei versus crystallization temperature: (□) sample A, (○) sample B, and (△) sample C.

CONCLUSIONS

In the reactor-made blends of PP and EPR, the presence of EPR affects the linear spherulite growth rate and crystal morphology of the PP matrix. The formation of T-lamellae is enhanced by the addition of EPR and, as a result, the blends show spherulites with positive birefringence in the wide range of isothermal crystallization temperature, while in homo-PP, only spherulites with negative birefringence are observed over the same range of temperature.

In these blends the presence of the sequentially copolymerized EPR hinders the crystallization of PP both in the nucleation and growth of the spherulites.

The authors thank Montell Polyolefins [Ferrara (I)] for supplying the materials.

REFERENCES

1. P. Galli, J. C. Haylock, and T. Simonazzi, in *Polypropylene: Structures, Blends and Composites, Copolymers and Blends,* Vol. 2, J. Karger-Kocsis, Ed., Chapman & Hall, London, 1995, Chap. 1.
2. P. Galli and J. C. Haylock, *Prog. Polym. Sci.,* **16,** 443 (1991).
3. E. Martuscelli, C. Silvestre, and G. Abate, *Polymer,* **23,** 229 (1982).
4. L. D'Orazio, C. Mancarella, E. Martuscelli, and G. Sticotti, *J. Mater. Sci.,* **26,** 4033 (1991).
5. E. Martuscelli, *Polym. Eng. Sci.,* **24,** 563 (1984).
6. R. Greco, E. Martuscelli, G. Ragosta, and Yin Jinghua, *J. Mater. Sci.,* **23,** 4307 (1988).

7. R. Greco, C. Mancarella, E. Martuscelli, G. Ragosta, and Yin Jinghua, *Polymer,* **28,** 1922 (1987).
8. Z. Bartczak, A. Galeski, and E. Martuscelli, *Polym. Eng. Sci.,* **24,** 1155 (1984).
9. Z. Bartczak, A. Galeski, E. Martuscelli, and H. Janik, *Polymer,* **26,** 1843 (1985).
10. P. Prentice, *Polymer,* **23,** 1189 (1982).
11. D. Yang, B. Zhang, Y. Yang, Z. Fang, G. Sun, and Z. Feng, *Polym. Eng. Sci.,* **24,** 612 (1984).
12. Z. Bartczak, A. Galeski, and E. Martuscelli, in *Polypropylene: Structures, Blends and Composites, Copolymers and Blends,* Vol. 2, J. Karger-Kocsis, Ed., Chapman & Hall, London, 1995, Chap. 2.
13. E. Martuscelli, in *Polypropylene: Structures, Blends, and Composites, Copolymers and Blends,* Vol. 2, J. Karger-Kocsis, Ed., Chapman & Hall, London, 1995, Chap. 4.
14. E. N. Kresge, in *Thermoplastic Elastomers,* G. Holden, N. R. Legg, R. Quirk, and H. E. Schoeder, Eds., Hanser Publishers, Munich, Vienna, and New York, 1996.
15. F. J. Padden, Jr. and H. D. Keith, *J. Appl. Phys.,* **10,** 1479 (1959).
16. D. R. Norton and A. Keller, *Polymer,* **26,** 704 (1985).
17. B. Lotz and J. C. Wittmann, *J. Polym. Sci., Polym. Phys.,* **24,** 1541 (1986).
18. F. J. Padden, Jr. and H. D. Keith, *J. Appl. Phys.,* **44,** 1217 (1973).
19. A. J. Lovinger, *J. Polym. Sci., Polym. Phys. Ed.,***21,** 97 (1983).
20. G. H. Meetin, *Optical Properties of Polymers,* Elsevier Applied Science Publishers, London and New York, 1986, p. 179.
21. J. J. Janimak, S. Z. D. Cheng, P. A. Giusti, and E. T. Hsieh, *Macromolecules,* **24,** 2253 (1991).
22. T. Kowalewski and A. Galeski, *J. Appl. Polym. Sci.,* **32,** 2919 (1986).